Sliding observer-based demagnetisation fault-tolerant control in permanent magnet synchronous motors

Changfan Zhang, Gongping Wu, Jing He, Kaihui Zhao

College of Electrical and Information Engineering, Hunan University of Technology, Zhuzhou, Hunan 412007, People's Republic of China
E-mail: hejing@263.net

Published in *The Journal of Engineering*; Received on 5th December 2016; Accepted on 19th April 2017

Abstract: This study proposes a fault-tolerant control method for permanent magnet synchronous motors (PMSMs) based on the active flux linkage concept, which addresses permanent magnet (PM) demagnetisation faults in PMSMs. First, a mathematical model for a PMSM is established based on active flux linkage, and then the effect of PM demagnetisation on the PMSM is analysed. Second, the stator current in the static coordinate is set as the state variable, an observer is designed based on a sliding-mode variable structure, and an equation for active flux linkage is established for dynamic estimation based on the equivalent control principle of sliding-mode variable structure. Finally, the active flux linkage for the next moment is predicted according to the operating conditions of the motor and the observed values of the current active flux linkage. The deadbeat control strategy is applied to eliminate errors in the active flux linkage and realise the objective of fault-tolerant control. A timely and effective control for demagnetisation faults is achieved using the proposed method, which validity and feasibility are verified by the simulation and experiment results.

1 Introduction

Permanent magnet synchronous motors (PMSMs) are widely used in the vehicle transportation systems today [1]. Compared to other kinds of motor used in the vehicle transportation systems, the PMSM is favourable for the advantages such as high efficiency, high power density, and large torque-to-weight ratio [2–4]. However, given the complex operating conditions, considerable environmental differences, and increase in service duration, the excitation performance of permanent magnets (PMs) may have declined to varying extents, thereby directly affecting motor performance and vehicle transportation systems [5]. To address this issue, conducting online detection and establishing a timely and effective control for PM demagnetisation faults are critical to guarantee a highly efficient and reliable operation of PMSMs in the vehicle transportation systems.

The PM demagnetisation faults greatly restrict the use of PMSMs. Wang *et al.* [6] proposed a novel approach for detecting and diagnosing partial demagnetisation fault in PMSMs operating under non-stationary conditions based on the tracking characteristic orders of stator current using the Vold–Kalman filter. Moon *et al.* [7] detected and estimated the severity of demagnetisation faults and calculated the varying inductance parameters using the least-squares method. This technique generates better results than the conventional methods for estimating flux linkages in PMSMs with a demagnetisation fault. Nair *et al.* [8] assessed the post-demagnetisation performance of interior PM AC machines by employing a highly accurate recoil line approach based on two-dimensional (2D) transient finite-element analysis. This method predicts post-fault machine performance and the phase currents required for a specific torque at any load conditions following a fault condition that leads to partial demagnetisation. Using the changes in torque spectrum and the track diagram of a torque ripple, Hong *et al.* [9] detected PM demagnetisation by analysing the characteristic quantity of the output torque for a motor under fault. Yoo *et al.* [10] proposed a demagnetisation diagnosis method based on locked rotor test results to detect PM demagnetisation through the locked-rotor torque and current of the motor. Accordingly, He *et al.* [11] proposed a robust demagnetisation fault detection method in PMSM based on sliding observer. Huang *et al.* [12] proposed an online PM demagnetisation faults detection method based on a minimum-order extended flux-linkage sliding-mode observer. These methods can effectively detect the PM demagnetisation faults, but cannot implement good control over it. Zhao *et al.* [13] proposed a robust PM flux-linkage non-singular fast terminal-sliding-mode observer to detect demagnetisation faults, which addresses irreversible demagnetisation of a PM for PMSMs. This method is only through the compensation of *d*-axis current to reduce the PM demagnetisation risk under the case of flux-weakening control, and it does not propose a fault-tolerant control method for PMSMs. The aforementioned methods can only be used to detect demagnetisation fault. However, PMSM is often stopped when addressing demagnetisation fault, thereby affecting the efficiency and quality of vehicle transportation systems.

In this paper, a method for demagnetisation fault detection and fault-tolerant control is proposed, which can effectively control and management of demagnetisation fault. The fault-tolerant control strategy maintains safe and reliable operations amid demagnetisation fault in PMSMs based on the real-time and accurate monitoring of the active flux linkage of the motor. To improve the dynamic performance and accuracy of the fault-tolerant control, we implemented the deadbeat control strategy. This control strategy is characterised by fast response and easy to implement in PMSM control systems.

This paper is organised as follows. The PM demagnetisation fault in PMSMs is analysed in Section 1. The fault-tolerant control algorithm is established in Section 2. A sliding-mode observer is designed in Section 3. The simulation and experiment results are provided and analysed in Section 4. The conclusions are drawn in Section 5.

2 Analysis of demagnetisation fault in the PMSM

2.1 Mathematical mode of the PMSM

The model of the PMSM is defined in the $(d\,q)$ coordinates as follows [14]:

Voltage equation

$$\begin{cases} u_d = Ri_d + \dfrac{\mathrm{d}\psi_d}{\mathrm{d}t} - \omega\psi_q \\ u_q = Ri_q + \dfrac{\mathrm{d}\psi_q}{\mathrm{d}t} + \omega\psi_d \end{cases} \tag{1}$$

This is an open access article published by the IET under the Creative Commons Attribution-NoDerivs License (http://creativecommons.org/licenses/by-nd/3.0/)

Flux equation

$$\begin{cases} \psi_d = \psi_{r0} + L_d i_d \\ \psi_q = L_q i_q \end{cases} \tag{2}$$

The electromagnetic torque produced by a PMSM can be described as

$$T_e = \frac{3}{2} n_p \left[\psi_{r0} + (L_d - L_q) i_d \right] i_q \tag{3}$$

The mechanical dynamics of the PMSM model is

$$T_e - T_L = J \frac{d\omega}{dt} \tag{4}$$

where u_d, u_q and i_d, i_q are the voltages and the currents in the (d q) coordinate, respectively, R is the stator resistance, L_d and L_q are d-axis and q-axis stator inductances, respectively, ψ_d and ψ_q are the $d-$axis and $q-$axis stator fluxes, respectively, ψ_{r0} and J are the flux produced by the PMs and the moment of inertia, respectively, and ω is the electrical rotor speed. n_p is the number of pole pairs, T_e is the electromagnetic torque and T_L is the load torque.

The active flux linkage is defined as [15, 16]

$$\psi_{ext} = \psi_{r0} + (L_d - L_q) i_d \tag{5}$$

The previous equation indicates that the active flux vector is aligned with the d-axis of the rotor frame. The active flux linkage is shown in Fig. 1.

The relation between the active flux linkage and the electromagnetic torque can be obtained when (5) is substituted into (3)

$$T_e = \frac{3}{2} n_p \psi_{ext} i_q \tag{6}$$

From (5) and (6), the active flux linkage ψ_{ext} is the total flux linkage on the rotor axle, which is used to generate torque in the electromagnetic torque equation.

2.2 Analysis of demagnetisation fault

Flux linkage will change when the PM motor operates because of external factors, such as temperature. The flux linkage for a PM will change from the original ψ_{r0} to ψ_r, and the active flux linkage will change to

$$\bar{\psi}_{ext} = |\psi_r| + (L_d - L_q) i_d \tag{7}$$

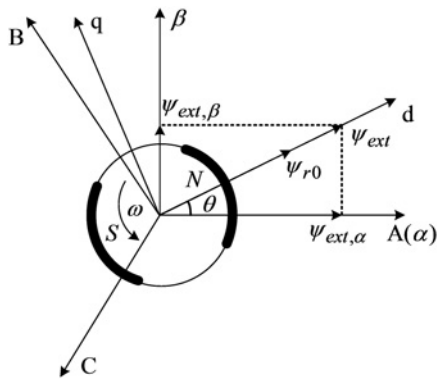

Fig. 1 *Definitions of active flux for PMSM*

The electromagnetic torque equation is transformed into

$$\bar{T}_e = \frac{3}{2} n_p \bar{\psi}_{ext} i_q \tag{8}$$

The control mode for $i_d = 0$ is mainly studied in this work. Therefore, when $i_d = 0$, then based on (5) and (7), the following expression is obtained:

$$\bar{\psi}_{ext} = \frac{|\psi_r|}{\psi_{r0}} \cdot \psi_{ext} = \lambda \cdot \psi_{ext} \tag{9}$$

where λ is the magnetic loss rate of the PM.

In case of PM demagnetisation faults, the following situation occurs based on (8). If the electromagnetic torque is maintained, and then the current on the q-axis will increase. Consequently, the actual current will vary from the given current and the current regulator will be saturated rapidly, thereby resulting in an uncontrollable current. An uncontrollable current may lead to over current, increase in DC voltage, poor torque performance of the motor or even uncontrollable motor behaviour and uncontrollable scrap. As indicated in (9), the active flux linkage is directly related to PM demagnetisation. That is, demagnetisation faults will directly result in changes in the active flux linkage, and the active flux linkage will generate the flux linkage for the electromagnetic torque. Therefore, the electromagnetic torque is maintained by keeping the active flux linkage constant.

3 Fault-tolerant control strategy

From the preceding analysis, the active flux linkage should be maintained to keep the electromagnetic torque constant in case of demagnetisation fault. However, the rotor of the PMSM consists of a PM, which cannot maintain the active flux linkage by regulating the magnet motive force. Consequently, maintaining the active flux linkage will rely only on current regulation.

3.1 Fault-tolerant control algorithm

Deadbeat control is a discretisation control strategy in which the actual values of the controlled volume can follow the given values after several or even one control period [17, 18]. From the preceding analysis, the active flux linkage generated under PM demagnetisation condition is unequal to the one generated under normal condition. To eliminate the influence of demagnetisation fault on the motor as soon as possible, theory of deadbeat control requires the expected value of the active flux linkage after PM demagnetisation occurred to follow the value under normal condition within one control period, thereby realising the objective of fault-tolerant control.

In case of PM demagnetisation fault, the weight relationship between the active flux linkage $\bar{\psi}_{ext}$ and the stator flux linkage on the d-axis and q-axis is expressed as follows:

$$\begin{cases} \psi_d = |\psi_r| + L_d i_d = \bar{\psi}_{ext} + L_q i_d \\ \psi_q = L_q i_q \end{cases} \tag{10}$$

From (10)

$$\begin{cases} i_d = \dfrac{\psi_d - \bar{\psi}_{ext}}{L_q} \\ i_q = \dfrac{\psi_q}{L_q} \end{cases} \tag{11}$$

This is an open access article published by the IET under the Creative Commons Attribution-NoDerivs License (http://creativecommons.org/licenses/by-nd/3.0/)

doi: 10.1049/joe.2016.0355

Equation (11) is substituted into (1)

$$\begin{bmatrix} \dot{\psi}_d \\ \dot{\psi}_q \end{bmatrix} = \begin{bmatrix} -\dfrac{R}{L_q} & \omega \\ -\omega & -\dfrac{R}{L_q} \end{bmatrix} \begin{bmatrix} \psi_d \\ \psi_q \end{bmatrix} + \begin{bmatrix} 1 & 0 \\ 0 & 1 \end{bmatrix} \begin{bmatrix} u_d \\ u_q \end{bmatrix} + \begin{bmatrix} \dfrac{R}{L_q} \bar{\psi}_{\text{ext}} \\ 0 \end{bmatrix} \tag{12}$$

The deadbeat control should be implemented in a discretisation field, such that discretisation should be conducted for (12)

$$\psi(k+1) = E\psi(k) + Fu(k) + P(k) \tag{13}$$

where T_s is the sampling period

$$\psi(k) = \begin{bmatrix} \psi_d(k) & \psi_q(k) \end{bmatrix}^{\text{T}}, \quad u(k) = \begin{bmatrix} u_d(k) & u_q(k) \end{bmatrix}^{\text{T}},$$

$$F = \begin{bmatrix} T_s & 0 \\ 0 & T_s \end{bmatrix}, \quad E = \begin{bmatrix} 1 - T_s \dfrac{R}{L_q} & T_s\omega \\ -T_s\omega & 1 - T_s \dfrac{R}{L_q} \end{bmatrix},$$

$$P(k) = \begin{bmatrix} T_s \dfrac{R}{L_q} \bar{\psi}_{\text{ext}}(k) \\ 0 \end{bmatrix}.$$

When (13) is used to predict the stator flux linkage, stator resistance and inductance on the q-axis of the motor are required to reduce their reliance on motor parameters. Moreover, (13) can be used to predict the salient pole or non-salient pole PMSM, which eliminates the salient pole phenomenon in the motor.

The active flux linkage is related to the weight of the stator flux linkage on the d-axis only. Therefore, only the weight of the flux linkage on the d-axis is considered. From (13)

$$\psi_d(k+1) = \left(1 - T_s \frac{R}{L_q}\right)\psi_d(k) + T_s\omega\psi_q(k) + T_s u_d(k) + T_s \frac{R}{L_q} \bar{\psi}_{\text{ext}}(k) \tag{14}$$

Discretisation shall be conducted for (10)

$$\begin{cases} \psi_d(k) = \bar{\psi}_{\text{ext}}(k) + L_q i_d(k) \\ \psi_q(k) = L_q i_q(k) \end{cases} \tag{15}$$

From (15), the weight of the stator flux linkage on the d-axis at moment $k+1$ is

$$\psi_d(k+1) = \bar{\psi}_{\text{ext}}(k+1) + L_q i_d(k+1) \tag{16}$$

When (15) and (16) are substituted into (14), the active flux linkage at moment $k+1$ is

$$\bar{\psi}_{\text{ext}}(k+1) = \bar{\psi}_{\text{ext}}(k) + \left(1 - T_s \frac{R}{L_q}\right) L_q i_d(k) + T_s\omega L_q i_q(k) + T_s u_d(k) - L_q i_d(k+1) \tag{17}$$

In accordance with the rules for deadbeat control, the active flux linkage at moment $k+1$ should be equal to the given value, i.e.

$$\bar{\psi}_{\text{ext}}(k+1) = \psi_{\text{ext}} \tag{18}$$

When (18) is substituted into (17), the predicted current value at moment $k+1$ is

$$i_d(k+1) = \frac{1}{L_q}\left[\bar{\psi}_{\text{ext}}(k) + L_q i_d(k) - T_s R i_d(k) + T_s\omega L_q i_q(k) + T_s u_d(k) - \psi_{\text{ext}}\right] \tag{19}$$

When the motor operates under normal condition, the current active flux linkage $\bar{\psi}_{\text{ext}}(k)$ is equal to the value under normal condition ψ_{ext}. From (19), $i_d(k+1) = 0$ is obtained and current on the d-axis should not be regulated. The active flux linkage $\bar{\psi}_{\text{ext}}(k)$ generated under PM demagnetisation condition is unequal to the value under normal condition ψ_{ext}. The current on the d-axis should be regulated to recover the active flux linkage $\bar{\psi}_{\text{ext}}(k+1)$ to a normal value at the next moment. The regulating volume is calculated as shown in (19).

3.2 Constraint conditions of the current

Therefore, maintaining active flux linkage should rely only on current regulation. Considering the stable operation of PMSM, the stator current cannot exceed the threshold limit value $I_{s\max}$ because of the limitation of the inverter output capacity and overload protection. Therefore, the following constraint condition should be satisfied when the current on the d-axis is adjusted

$$-I_{d\min} = -\sqrt{I_{s\max}^2 - i_q^2} < i_d$$

4 Design of state observer and fault reconstruction

As indicated in (19), the active flux linkage values of the current are required to achieve a regulating variable for the current on the d-axis after PM demagnetisation. As active flux cannot be measured, the observer must be designed.

When the PM on the rotor demagnetises, let $\bar{\psi}_{\text{ext},d}$ and $\bar{\psi}_{\text{ext},q}$ represent the active flux linkage components in the (d q) coordinates, we have

$$\begin{cases} \bar{\psi}_{\text{ext},d} = \psi_d - L_q i_d = \bar{\psi}_{\text{ext}} \\ \bar{\psi}_{\text{ext},q} = \psi_q - L_q i_q = 0 \end{cases} \tag{20}$$

From (20), (21) can be obtained

$$\begin{cases} \psi_d = \bar{\boldsymbol{\psi}}_{\text{ext},d} + L_q i_d \\ \psi_q = \bar{\boldsymbol{\psi}}_{\text{ext},q} + L_q i_q \end{cases} \tag{21}$$

Substituting (21) into (1)

$$\begin{bmatrix} u_d \\ u_q \end{bmatrix} = \begin{bmatrix} R & -\omega L_q \\ \omega L_q & R \end{bmatrix} \begin{bmatrix} i_d \\ i_q \end{bmatrix} + \begin{bmatrix} L_q & 0 \\ 0 & L_q \end{bmatrix} \begin{bmatrix} \dot{i}_d \\ \dot{i}_q \end{bmatrix} + \begin{bmatrix} 0 & -\omega \\ \omega & 0 \end{bmatrix} \begin{bmatrix} \bar{\boldsymbol{\psi}}_{\text{ext},d} \\ \bar{\boldsymbol{\psi}}_{\text{ext},q} \end{bmatrix} + \begin{bmatrix} \dot{\bar{\psi}}_{\text{ext},d} \\ \dot{\bar{\psi}}_{\text{ext},q} \end{bmatrix} \tag{22}$$

By using coordinate inversion, the voltage (22) in the stationary reference (α β) frame is transformed to be

$$\begin{bmatrix} u_\alpha \\ u_\beta \end{bmatrix} = \begin{bmatrix} R & 0 \\ 0 & R \end{bmatrix} \begin{bmatrix} i_\alpha \\ i_\beta \end{bmatrix} + \begin{bmatrix} L_q & 0 \\ 0 & L_q \end{bmatrix} \begin{bmatrix} \dot{i}_\alpha \\ \dot{i}_\beta \end{bmatrix} + \begin{bmatrix} \dot{\bar{\psi}}_{\text{ext},\alpha} \\ \dot{\bar{\psi}}_{\text{ext},\beta} \end{bmatrix} \tag{23}$$

This is an open access article published by the IET under the Creative Commons Attribution-NoDerivs License (http://creativecommons.org/licenses/by-nd/3.0/)

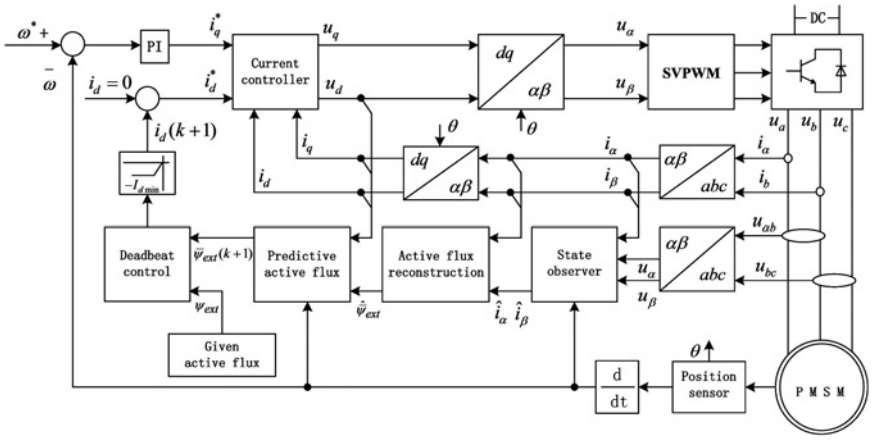

Fig. 2 *Diagram of fault-tolerant control for PMSM*

With

$$\begin{bmatrix} \bar{\psi}_{\text{ext},\alpha} \\ \bar{\psi}_{\text{ext},\beta} \end{bmatrix} = \bar{\psi}_{\text{ext}} \begin{bmatrix} \cos\theta \\ \sin\theta \end{bmatrix} \tag{24}$$

The time constant of the mechanical system is larger than that of the electrical system, and thus, we can assume that $\dot{\omega} = 0$. Moreover, the differential for the axis weight of the active flux linkage ($\alpha\beta$) is indicated as follows:

$$\begin{bmatrix} \dot{\bar{\psi}}_{\text{ext},\alpha} \\ \dot{\bar{\psi}}_{\text{ext},\beta} \end{bmatrix} = \omega\bar{\psi}_{\text{ext}} \begin{bmatrix} -\sin\theta \\ \cos\theta \end{bmatrix} = \begin{bmatrix} 0 & -\omega \\ \omega & 0 \end{bmatrix} \begin{bmatrix} \bar{\psi}_{\text{ext},\alpha} \\ \bar{\psi}_{\text{ext},\beta} \end{bmatrix} \tag{25}$$

Equations (23) and (25) are applied to develop a state equation for PMSM, as shown in (26). Only the stator resistance and inductance on the q-axis are included in the model, which reduces the influences of the parameters and eliminates the salient pole phenomenon of the motor

$$\dot{x} = Ax + Bu + D\bar{f}_a \tag{26}$$

where

$$u = \begin{bmatrix} u_\alpha & u_\beta \end{bmatrix}^{\text{T}}; \quad x = \begin{bmatrix} i_\alpha & i_\beta \end{bmatrix}^{\text{T}};$$

$$A = \begin{bmatrix} -\dfrac{R}{L_q} & 0 \\ 0 & -\dfrac{R}{L_q} \end{bmatrix}; \quad B = \begin{bmatrix} \dfrac{1}{L_q} & 0 \\ 0 & \dfrac{1}{L_q} \end{bmatrix};$$

$$D = \begin{bmatrix} 0 & \dfrac{\omega}{L_q} \\ -\dfrac{\omega}{L_q} & 0 \end{bmatrix} \bar{f}_a = \begin{bmatrix} \bar{\psi}_{\text{ext},\alpha} \\ \bar{\psi}_{\text{ext},\beta} \end{bmatrix};$$

The sliding-mode observer designed according to the system described by (26) is as follows:

$$\dot{\hat{x}} = A\hat{x} + Bu + \boldsymbol{k}\text{sgn}(x - \hat{x}) \tag{27}$$

where $\hat{x}$ is the observed value of x, $v = \boldsymbol{k}\text{sgn}(x - \hat{x})$ is sliding control item, sgn($\cdot$) is a sign function, $\boldsymbol{k}$ is the designed matrix, and $\boldsymbol{k} = \begin{bmatrix} k_1 & 0 \\ 0 & k_2 \end{bmatrix}$, $k_1 > 0$, $k_2 > 0$, the sliding surface is selected as $e = x - \hat{x} = \begin{bmatrix} e_1 \\ e_2 \end{bmatrix} = \begin{bmatrix} i_\alpha - \hat{i}_\alpha \\ i_\beta - \hat{i}_\beta \end{bmatrix}$.

Table 1 Nominal value of the motor parameters

Parameter	Values
stator resistance (R_s)	0.02 Ω
pole pairs (p)	4
inductance (d-axis) (L_d)	0.001 H
inductance (q-axis) (L_q)	0.003572 H
rotor flux (ψ_{f0})	0.892 Wb
inertia coefficient (J)	100 kg m^2

From (26) and (27), then

$$\dot{e} = \dot{x} - \dot{\hat{x}} = Ae + D\bar{f}_a - k\text{sgn}(e) \tag{28}$$

When $\boldsymbol{k}$ is satisfied, e will make a global asymptotic convergence to zero.

The convergence of observer can be verified as follows:

Proof: Consider the Lyapunov function

$$V = \frac{1}{2}e^{\text{T}}e \tag{29}$$

From (28) and (29), then

$$\begin{aligned} \dot{V} =& \text{e}^{\text{T}}(Ae + D\bar{f}_a - k\text{sgn}(e)) \\ =& \text{e}^{\text{T}}Ae + \text{e}^{\text{T}}D\bar{f}_a - \text{e}^{\text{T}}k\text{sgn}(e) \\ =& \begin{bmatrix} e_1 & e_2 \end{bmatrix} \begin{bmatrix} -\dfrac{R}{L_q} & 0 \\ 0 & -\dfrac{R}{L_q} \end{bmatrix} \begin{bmatrix} e_1 \\ e_2 \end{bmatrix} + \text{e}^{\text{T}}D\bar{f}_a - \text{e}^{\text{T}}\boldsymbol{k}\text{sgn}(e) \\ =& -\frac{R}{L_q}e_1^2 - \frac{R}{L_q}e_2^2 + \text{e}^{\text{T}}D\bar{f}_a - \text{e}^{\text{T}}\boldsymbol{k}\text{sgn}(e) \\ \le& \text{e}^{\text{T}}D\bar{f}_a - k_1\|e_1\| - k_2\|e_2\| \\ \le& \|e\|\|D\|\left\|\bar{f}_a\right\| - k_3\|e\| = \|e\|(\|D\|\left\|\bar{f}_a\right\| - k_3) \end{aligned} \tag{30}$$

where $k_3 = \min\{k_1, k_2\}$.

From an engineering point of view, the PM flux linkage should be bounded. Accordingly, the demagnetisation fault $\bar{f}_a$ can be assumed to be bounded, i.e. there exists a normal value F that satisfies

This is an open access article published by the IET under the Creative Commons Attribution-NoDerivs License (http://creativecommons.org/licenses/by-nd/3.0/)

doi: 10.1049/joe.2016.0355

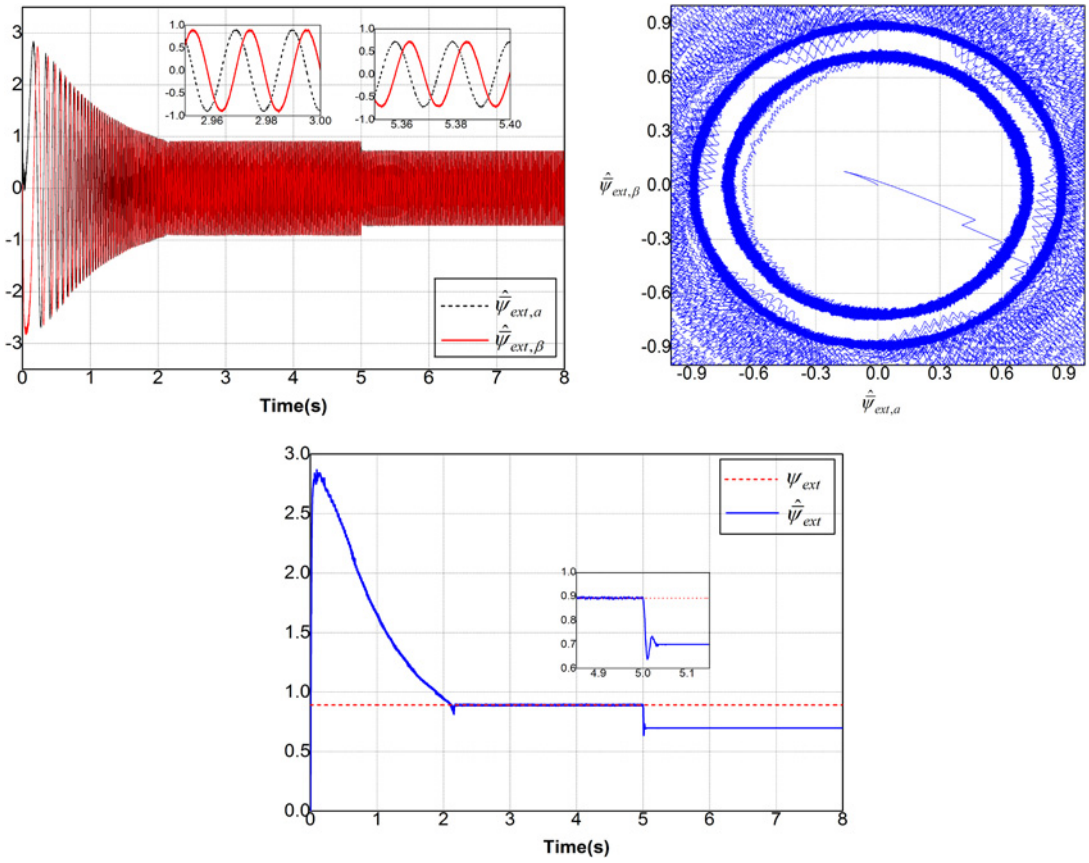

Fig. 3 *Observation of the active flux*

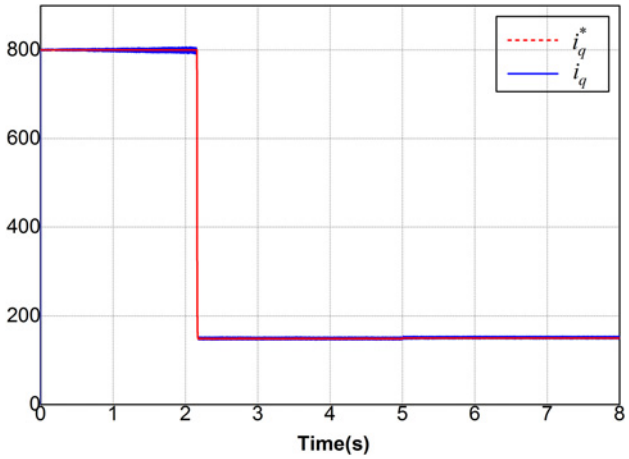

Fig. 4 *Simulation results of q-axis current response*

$\left\|\bar{f}_a\right\| \le F$. Suppose k_3 meets the condition of $k_3 \ge F\|D\| + \eta$, where $\eta \ge 0$, then $\dot{V} \le -\eta\|e\|$.

This completes the proof. □

When the system reaches the sliding mode surface, according to the sliding mode equivalent principle [11], i.e. $e = \dot{e} = 0$. It is assumed that $\begin{bmatrix} k_1 & k_2 \end{bmatrix}^{\mathrm{T}} = \omega\begin{bmatrix} \bar{k}_1 & \bar{k}_2 \end{bmatrix}^{\mathrm{T}}$, where $k_1 > 0$, $k_2 > 0$, From (28), the following equation is obtained:

$$\begin{cases} \bar{\psi}_{\mathrm{ext},\alpha} = -L_q \bar{k}_2 \mathrm{sgn} e_2 \\ \bar{\psi}_{\mathrm{ext},\beta} = L_q \bar{k}_1 \mathrm{sgn} e_1 \end{cases} \tag{31}$$

To reduce chattering in the sliding mode, a sign function can be used to replace the continuous function to construct the following reconstructing algorithm of the active flux linkage:

$$\begin{cases} \hat{\bar{\psi}}_{\mathrm{ext},\alpha} = -L_q \bar{k}_2 \dfrac{(i_\beta - \hat{i}_\beta)}{\left|i_\beta - \hat{i}_\beta\right| + \delta_2} \\ \hat{\bar{\psi}}_{\mathrm{ext},\beta} = L_q \bar{k}_1 \dfrac{(i_\alpha - \hat{i}_\alpha)}{\left|i_\alpha - \hat{i}_\alpha\right| + \delta_1} \end{cases} \tag{32}$$

where δ_1 and δ_2 are a small constant greater than zero.

From (24), the active flux linkage can be obtained

$$\hat{\bar{\psi}}_{\mathrm{ext}} = \sqrt{\hat{\bar{\psi}}^2_{\mathrm{ext},\alpha} + \hat{\bar{\psi}}^2_{\mathrm{ext},\beta}} \tag{33}$$

5 Simulation and experimental results

5.1 Diagram of the fault-tolerant control system for a PMSM

Fig. 2 shows the diagram of the structure of the fault-tolerant control system for the PMSM used in the simulation and the experiment. $i_d = 0$ the control strategy is applied in this system. The stator current (i_α, i_β), stator voltage (u_α, u_β), and rotational speed ω are inputted into the state observer module and outputted as the observed value for the stator current ($\hat{i}_\alpha$, $\hat{i}_\beta$). For the stator current (i_α, i_β) and the observed value ($\hat{i}_\alpha$, $\hat{i}_\beta$), the observed value of the active flux linkage $\hat{\bar{\psi}}_{\mathrm{ext}}$ is obtained using (32) and (33) in the reconstruction model for the active flux linkage. The current regulating volume values for the active flux linkage prediction module and the deadbeat control module are calculated using (19) under the

This is an open access article published by the IET under the Creative Commons Attribution-NoDerivs License (http://creativecommons.org/licenses/by-nd/3.0/)

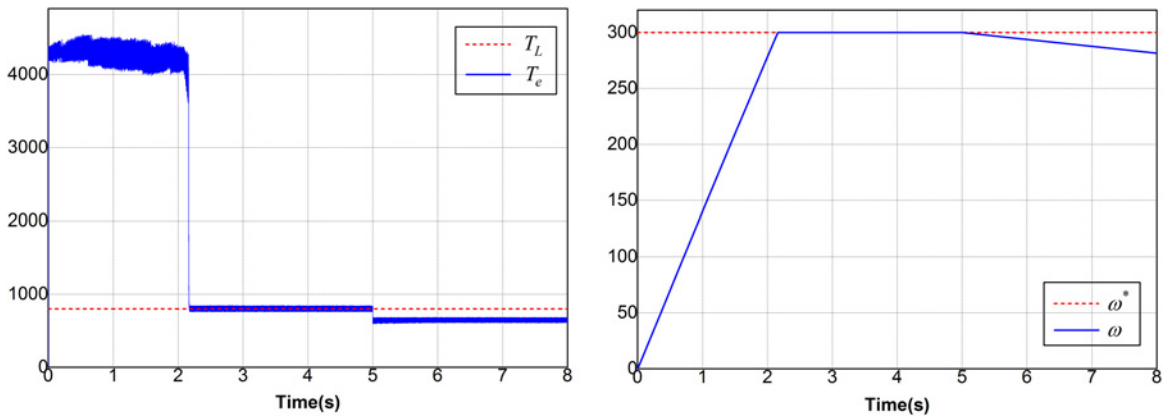

Fig. 5 *Simulation results of the torque and speed*

present operating conditions of the motor and the observed value of the active flux linkage $\hat{\bar{\psi}}_{\text{ext}}$.

The motor parameters used for the simulation and the experiment are listed in Table 1. The simulation is conducted in MATLAB/Simulink, and the sampling frequency is set as 10 kHz. The DC voltage is 1500 V, and the amplitude value of the stator current is 350 A. The percentage and integral coefficient of the rotational speed proportional–integral regulator are 2000 and 0.5, respectively. Moreover, the parameters for the observer and the fault reconstruction module are $k_1 = k_2 = 500$ and $\delta_1 = \delta_2 = 0.01$, respectively. The given values for the active flux linkage, rotational speed, and load torque are 0.892 Wb, $\omega^* = 300$ rad/s, and $T_{\text{L}} = 800$ N, respectively. The actual dynamic change for magnetic loss in the motor cannot be simulated easily, and thus, the method of setting a nominal deviation of the flux linkage is applied to simulate magnetic loss. The nominal value for the flux linkage is set from 0.892 to 0.7 Wb at a time of 5 s.

5.2 *Without the fault-tolerant control algorithm*

The simulation results are obtained under PM demagnetisation condition and without the fault-tolerant control algorithm. Fig. 3 shows the observation results of the active flux linkage for the motor. Before 5 s, the mean value of the stable estimation results for $\hat{\bar{\psi}}_{\text{ext},\alpha}$, $\hat{\bar{\psi}}_{\text{ext},\beta}$, and the active flux linkage is 0.892 Wb; after 5 s, the mean value is 0.7 Wb. As shown in the figure, the sine degree of the flux linkage viewed from the sliding-mode observer under a stable condition is good, and the relative error is small. The phase angle between $\hat{\bar{\psi}}_{\text{ext},\alpha}$ and $\hat{\bar{\psi}}_{\text{ext},\beta}$ is basically 90°.

The theoretical calculation indicates that:

Before 5 s, $\hat{\bar{\psi}}_{\text{ext},\alpha} = 0.892\cos\theta$, $\hat{\bar{\psi}}_{\text{ext},\beta} = 0.892\sin\theta$, and $\hat{\bar{\psi}}_{\text{ext}} = \sqrt{\hat{\bar{\psi}}_{\text{ext},\alpha}^2 + \hat{\bar{\psi}}_{\text{ext},\beta}^2} = 0.892$. From $(\hat{\bar{\psi}}_{\text{ext},\alpha} - 0)^2 + (\hat{\bar{\psi}}_{\text{ext},\beta} - 0)^2 = 0.892^2$, the active flux linkage under a stable condition operates around the circle with a radius of 0. 892 and (0, 0) as the centre.

After 5 s, $\hat{\bar{\psi}}_{\text{ext},\alpha} = 0.7\cos\theta$, $\hat{\bar{\psi}}_{\text{ext},\beta} = 0.7\sin\theta$, and $\hat{\bar{\psi}}_{\text{ext}} = \sqrt{\hat{\bar{\psi}}_{\text{ext},\alpha}^2 + \hat{\bar{\psi}}_{\text{ext},\beta}^2} = 0.7$. From $(\hat{\bar{\psi}}_{\text{ext},\alpha} - 0)^2 + (\hat{\bar{\psi}}_{\text{ext},\beta} - 0)^2 = 0.7^2$, the active flux linkage under a stable condition operates around the circle with a radius of 0. 7 and (0, 0) as the centre.

A comparison shows that the observed results of the active flux linkage are consistent with the theoretical analysis results, thereby indicating that the designed sliding-mode observer can accurately observe the active flux linkage in real time and reduce the active flux linkage after PM demagnetisation.

To validate PM demagnetisation and the influence of the active flux linkage on electromagnetic torque, the current on the q-axis is limited to maintain its value before and after PM demagnetisation, as shown in Fig. 4. The waveforms of the electromagnetic torque and the rotational speed are shown in Fig. 5. The simulation results indicate that PM demagnetisation occurs and the active flux linkage is reduced, thereby resulting in the decline of the electromagnetic torque and the slow operation of the motor.

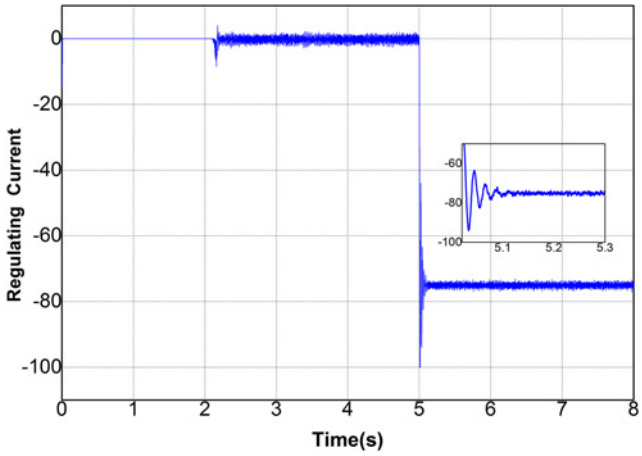

Fig. 6 *Simulation results of regulating current*

5.3 *Fault-tolerant control algorithm*

The simulation results are obtained under PM demagnetisation condition and with the fault-tolerant control algorithm. Fig. 6 shows the regulating current from the deadbeat control module. To prevent the effect of current on the control system during the motor starting stage, the regulating current is limited to zero. As shown in the figure, when the motor operates under normal condition, the output regulating current is zero. After 5 s, magnetic loss occurs in the motor and the regulating current should be the output to maintain the active flux linkage. The stable state value for the regulating current is −75.1 A, whereas the theoretical calculation value is −74.6 A, from which the fault-tolerant control algorithm can be used to calculate the regulating current accurately. When the load torque is 800 N, the constraint value for the current on the d-axis is −318 A, which is limited within the constraint scope for the regulating current. Fig. 7 shows the observed results of the active flux linkage after adding the fault-tolerant control algorithm. As shown in the figure, the deadbeat module after 5 s is inputted into the regulating current. Moreover, the active flux linkage for the motor is recovered to the value under normal condition. Fig. 8 shows the current waveform. $i_d = 0$ is applied as the control strategy, and the regulating current after 5 s is given current on the d-axis. As shown in the figure, the regulating

This is an open access article published by the IET under the Creative Commons Attribution-NoDerivs License (http://creativecommons.org/licenses/by-nd/3.0/)

doi: 10.1049/joe.2016.0355

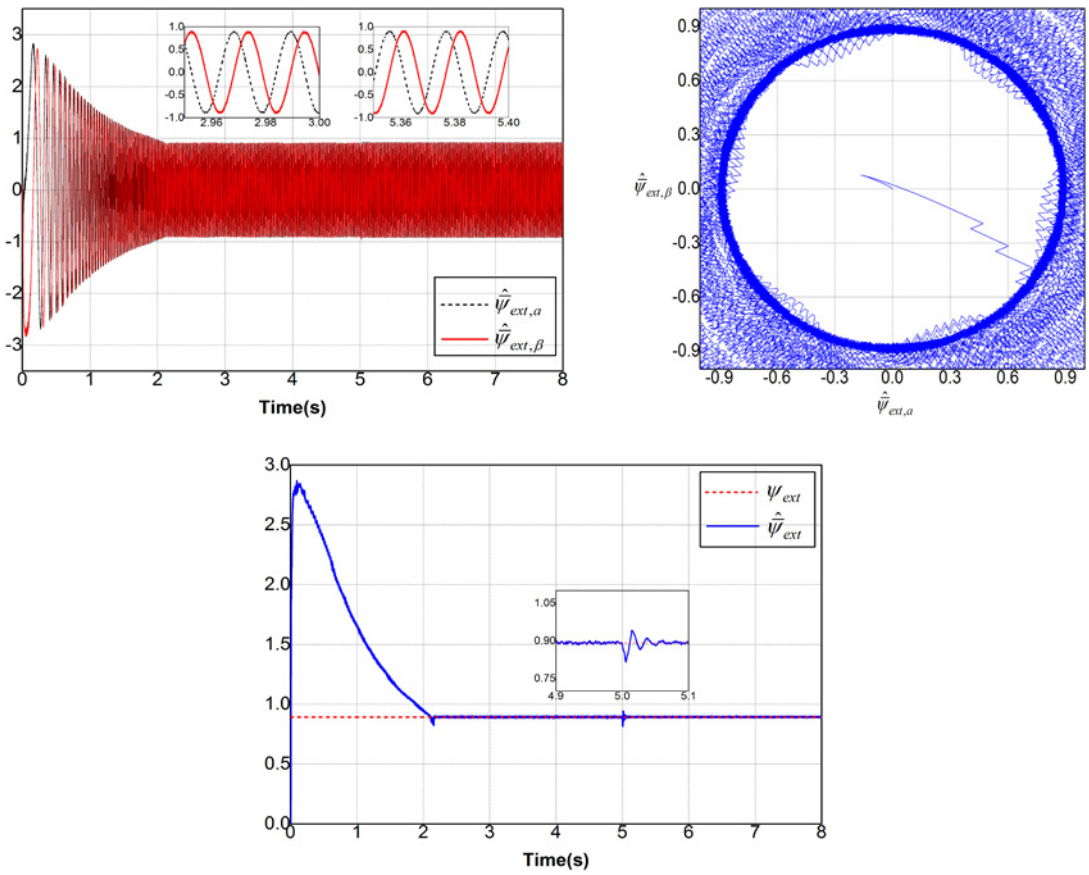

Fig. 7 *Observation of the active flux*

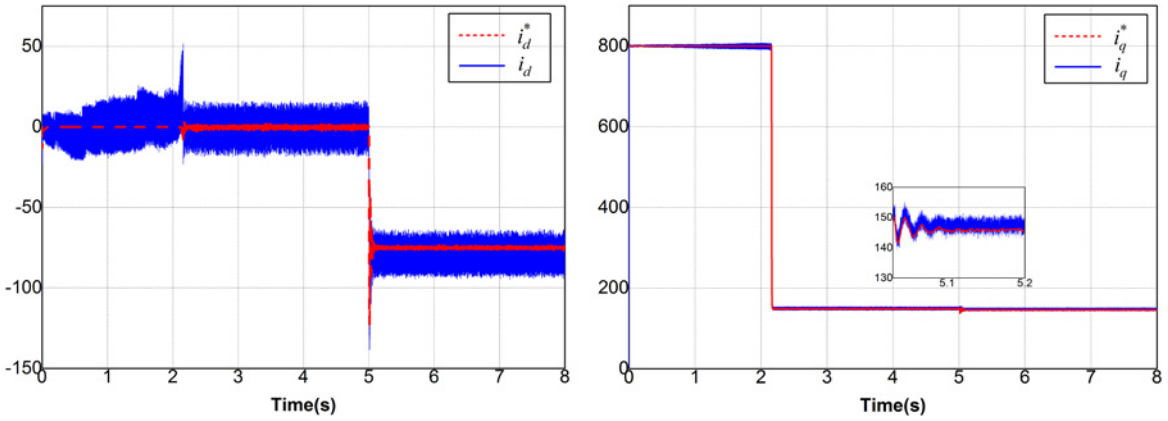

Fig. 8 *Simulation results of current response*

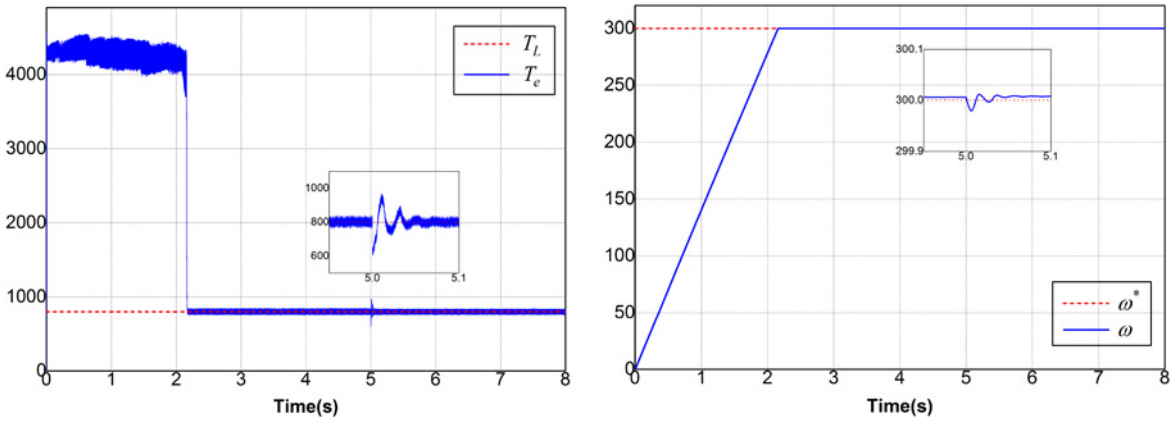

Fig. 9 *Simulation results of torque and speed*

doi: 10.1049/joe.2016.0355
This is an open access article published by the IET under the Creative Commons Attribution-NoDerivs License (http://creativecommons.org/licenses/by-nd/3.0/)

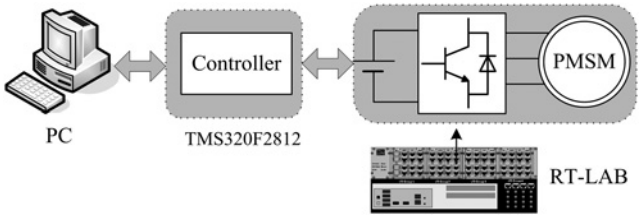

Fig. 10 *Configuration of the RT-Lab hardware-in-the-loop simulation system*

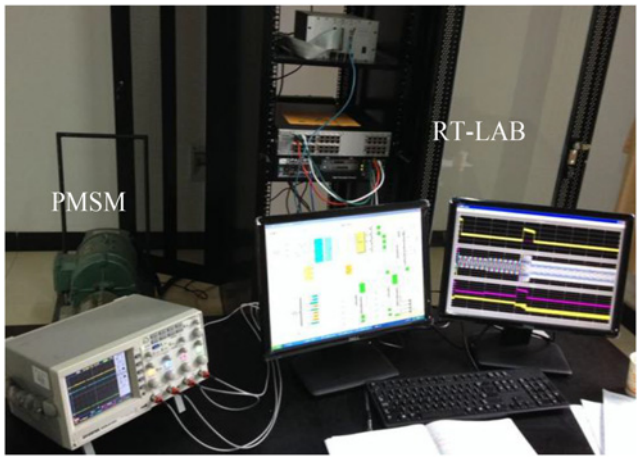

Fig. 11 *RT-Lab experiment setup*

current on the *d*-axis can mitigate the continuous increase of the large current on the *q*-axis, thereby resulting in an uncontrollable current. The electromagnetic torque and rotational speed waveforms after adding the fault-tolerant control algorithm are shown in Fig. 9. Therefore, the electromagnetic torque is maintained and the motor operates steadily after adding the fault-tolerant control algorithm (Fig. 10).

5.4 Experimental results

The experiment is composed by DSP controller, OP5600 simulation motor, related cables, multi-motor system model as software component and upper computer monitoring interface, as shown in Fig. 11. The actual DSP controller TMS320F2812 is used in the experimental system. PMSM is simulated by RT-lab (OP5600). The configuration is shown in Fig. 10, and the experimental results are shown in Figs. 12 and 13.

The experimental results without the fault-tolerant control algorithm are presented in Fig. 12. As shown in Figs. 12*a* and *b*, the active flux linkage for the motor with PM demagnetisation will decline. When the active flux linkage is reduced, the electromagnetic torque will decline and the motor will operate slowly, as shown in Fig. 12*c*. The experimental results with the fault-tolerant control algorithm are presented in Fig. 13. As shown in Figs. 13*a* and *b*, the active flux linkage for the motor is recovered to the value under normal condition when the regulating current is the output for the deadbeat control module, thereby preventing the generation of an uncontrollable current on the *q*-axis. After adding the fault-tolerant control algorithm, the electromagnetic torque is maintained and the motor operates steadily, as shown in Fig. 13*c*.

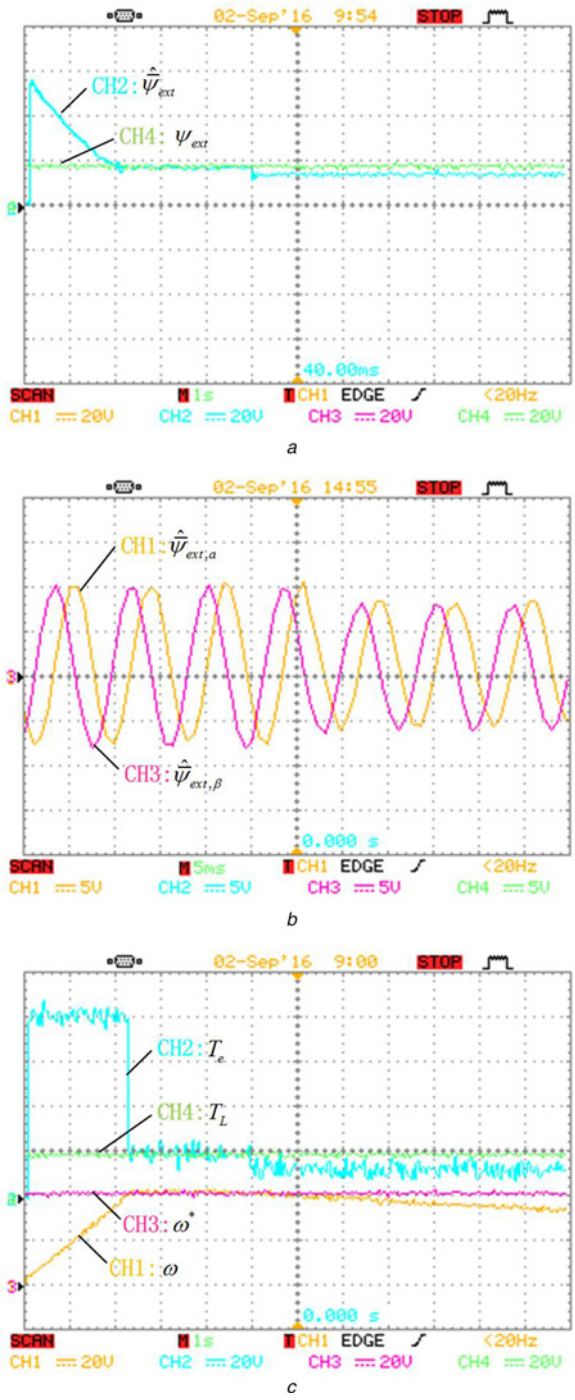

Fig. 12 *Experimental wave forms of without the fault-tolerant control*
a $\hat{\psi}_{ext}$, ψ_{ext}: 1 Wb/div
b $\hat{\psi}_{ext,\alpha}$, $\hat{\psi}_{ext,\beta}$: 0.25 Wb/div
c ω, ω^*: 150 rad/s/div; T_e, T_L: 1000 N/div

6 Conclusion

A method for demagnetisation fault detection and fault-tolerant control for PMSMs was proposed based on the active flux linkage concept. The following conclusions can be drawn from the proposed method:

i. Regardless of whether the PM is under fault or normal operation, the proposed sliding-mode observer can accurately observe the active flux linkage of the motor. Moreover, only the stator resistance and induction on the *q*-axis are necessary for the observer.
ii. When the PM operates under fault condition, the proposed method can regulate the current on the *d*-axis in a timely manner and recover the active flux linkage under fault condition to the value under normal condition. The simulation and experiment

This is an open access article published by the IET under the Creative Commons Attribution-NoDerivs License (http://creativecommons.org/licenses/by-nd/3.0/)

doi: 10.1049/joe.2016.0355

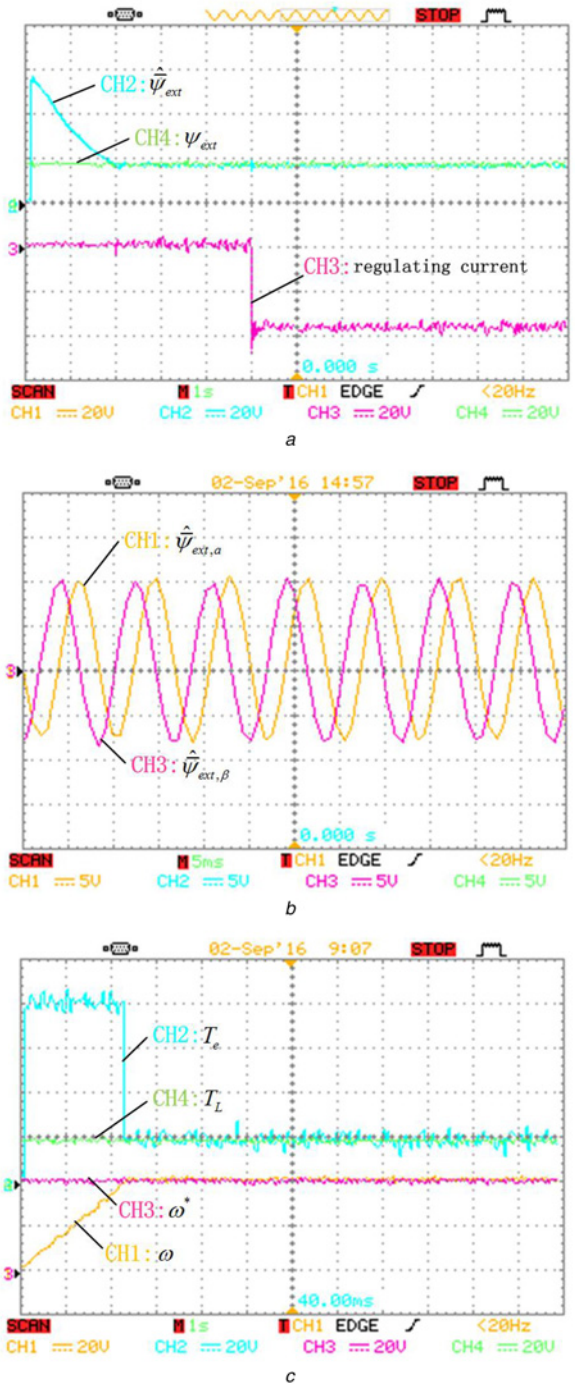

Fig. 13 *Experimental wave forms of fault-tolerant control*
a $\hat{\psi}_{ext}$, ψ_{ext}: 1 Wb/div; regulating current: 40 A/div
b $\hat{\psi}_{ext,\alpha}$, $\hat{\psi}_{ext,\beta}$: 0.25 Wb/div
c ω, ω^*: 150 rad/s/div; T_e, T_L: 1000 N/div

results show that the electromagnetic torque is maintained and that the motor operates steadily after adding the fault-tolerant control algorithm.

iii. The proposed fault-tolerant control method does not highly depend on the motor parameters and can also be applied to non-salient pole PMSMs. This method can expand the applications of PMSMs under poor conditions and other situations with high reliability requirements.

7 Acknowledgements

This work was supported by the Natural Science Foundation of China (no. 61473117), Hunan Provincial Natural Science Foundation of China (nos. 2016JJ5012 and 2017JJ4031), Scientific Research Fund of the Hunan Provincial Education Department (no. 16A058), Key Laboratory for Electric Drive Control and Intelligent Equipment of Hunan Province, and Science and Technology Innovative Research Team in Higher Educational Institutions of Hunan Province.

8 References

[1] Reitz M., Wang X., Gu P.: 'Robust sliding mode control of permanent magnet synchronous motor drives'. IEEE Transportation Electrification Conf. (ITEC), 2016, pp. 1–6
[2] Morimoto S., Ooi S., Inoue Y., *ET AL.*: 'Experimental evaluation of a rare-earth-free PMASynRM with ferrite magnets for automotive applications', *IEEE Trans. Ind. Electron.*, 2014, **61**, pp. 5749–5756
[3] Khanchoul M., Hilairet M., Normand-Cyrot D.: 'A passivity-based controller under low sampling for speed control of PMSM', *Control Eng. Pract.*, 2014, **26**, pp. 20–27
[4] Su K., Li C.: 'Chaos control of permanent magnet synchronous motors via unidirectional correlation', *Int. J. Light Electron Opt.*, 2014, **125**, pp. 3693–3696
[5] Vinson G., Combacau M., Prado T.: 'Permanent magnets synchronous machines faults detection and identification'. 38th Annual Conf. of the IEEE Industrial Electronics Society (IECON), 2012, pp. 3925–3930
[6] Wang C., Delgado M., Romeral L., *ET AL.*: 'Detection of partial demagnetization fault in PMSMs operating under nonstationary conditions', *IEEE Trans. Magn.*, 2016, **2**, pp. 1–4
[7] Moon S., Lee J., Jeong H., *ET AL.*: 'Demagnetization fault diagnosis of a PMSM based on structure analysis of motor inductance', *IEEE Trans. Ind. Electron.*, 2016, **63**, pp. 3795–3803
[8] Nair S.S., Patel V.I., Wang J.: 'Post-demagnetization performance assessment for interior permanent magnet AC machines', *IEEE Trans. Magn.*, 2016, **52**, pp. 1–10
[9] Hong J., Park S., Doosoo H.: 'Detection and classification of rotor demagnetization and eccentricity faults for PM synchronous motors', *IEEE Trans. Ind. Appl.*, 2012, **48**, pp. 923–932
[10] Yoo J.H., Hwang D.H., Jung T.U.: 'Irreversible demagnetization fault diagnosis of permanent magnet synchronous motor for electric vehicle'. IEEE Vehicle Power and Propulsion Conf. (VPPC), Montreal, Canada, 2015, pp. 1–4
[11] He J., Zhang C.F., Mao S.G., *ET AL.*: 'Demagnetization fault detection in permanent magnet synchronous motors based on sliding observer', *J. Nonlinear Sci.*, 2016, **29**, pp. 2039–2048
[12] Huang G., Luo Y.P., Zhang C.F., *ET AL.*: 'Online demagnetization detection of permanent magnet synchronous traction motor based on extended flux linkage', *J. Chin. Railway Soc.*, 2016, **38**, pp. 48–55
[13] Zhao K.H., Chen T.F., Zhang C.F., *ET AL.*: 'Online fault detection of permanent magnet demagnetization for IPMSMs by non-singular fast terminal-sliding-mode observer', *Sensors*, 2014, **14**, pp. 23119–23136
[14] Lin W., Liu D., Wu Q., *ET AL.*: 'Comparative study on direct torque control of interior permanent magnet synchronous motor for electric vehicle', *Int. Federation Autom. Control (IFAC)*, 2015, **48**, pp. 65–71
[15] Boldea I., Paicu M.C., Andreescu G.D.: "Active flux' DTFC-SVM Sensor Less Control of IPMSM', *IEEE Trans. Energy Convers.*, 2009, **24**, pp. 314–322
[16] Huang G., Luo Y.P., Zhang C.F., *ET AL.*: 'Current sensor fault reconstruction for PMSM drives', *Sensors*, 2016, **3**, pp. 1–16
[17] Turker T., Buyukkeles U., Bakan A.F.: 'A robust predictive current controller for PMSM drives', *IEEE Trans. Ind. Electron.*, 2016, **63**, pp. 3906–3914
[18] Buso S., Caldognetto T., Brandao D.I.: 'Dead-beat current controller for voltage-source converters with improved large-signal response', *IEEE Trans. Ind. Appl.*, 2016, **52**, pp. 1588–1596

This is an open access article published by the IET under the Creative Commons Attribution-NoDerivs License (http://creativecommons.org/licenses/by-nd/3.0/)